International Journal of Engineering, Mathematical and Physical Sciences
ISSN: 2517-9934
Vol:7, No:6, 2013

Analysis of Thermal Deformation of a Rough Slider and Its Asperities and Its Impact on Load Generation in Parallel Sliders

Prawal Sinha and Getachew Adamu

***Abstract*—**Heating is inevitable in any bearing operation. This leads to not only the thinning of the lubricant but also could lead to a thermal deformation of the bearing. The present work is an attempt to analyze the influence of thermal deformation on the thermo-hydrodynamic lubrication of infinitely long tilted pad slider rough bearings. As a consequence of heating the slider is deformed and is assumed to take a parabolic shape. Also the asperities expand leading to smaller effective film thickness. Two different types of surface roughness are considered: longitudinal roughness and transverse roughness. Christensen's stochastic approach is used to derive the Reynolds-type equations. Density and viscosity are considered to be temperature dependent. The modified Reynolds equation, momentum equation, continuity equation and energy equation are decoupled and solved using finite difference method to yield various bearing characteristics. From the numerical simulations it is observed that the performance of the bearing is significantly affected by the thermal distortion of the slider and asperities and even the parallel sliders seem to carry some load.

***Keywords*—**Thermal Deformation, Tilted pad slider bearing, longitudinal roughness, transverse roughness, load capacity.

I. Introduction

SEVERAL research works have been done to investigate the thermal effects and surface roughness effects on the performance of tilted pad slider bearings. Several researchers such as Fogg [1], Osterle et al [2], Lewicki [3], Cameron [4], Young [5], Lebeck [6], etc. have experimentally investigated the thermal influence on the load carrying capacity of parallel slider bearings. The results of all these researchers show the existence of a lifting force (load capacity) even when parallel bearings are in operation. However, the precise causes which are responsible for this phenomenon are not precisely understood. Zienkiewicz [7] considered the slider and pad at different temperatures and showed that for parallel slider bearing if the pad temperature is greater than the slider temperature then a suctional effect, which may lead to a drastic fall in load carrying capacity, is possible. Rodkiewicz and Sinha [8] provided an orderly analysis which elaborates on the mechanisms that may be responsible for the fluid generated lifting force. It is indicated that the consideration of the fore region pressure together with the density variation may lead to a useful load support with a reduced friction, even for parallel sliding bearing.

Thermohydrodynamic lubrication problems of slider bearings have been analyzed numerically by many researchers such as Ezzat and Rhode [9], Pinkus [10], Kumar et al. [11]. A detailed review can be found in a paper by Khonsari [12].

Tzeng and Saibel [13] have introduced stochastic concepts to analyze a two dimensional inclined slider bearing with one dimensional roughness in the direction transverse to the sliding direction. Using the same approach Christensen and Tonder [14] and Christensen [15] analyzed two types of one dimensional roughness: longitudinal roughness and transverse roughness models of hydrodynamic lubrication of tilted pad slider bearings. They developed a modified Reynolds equation applicable to each of these models and used to analyze the behavior of a fixed pad slider bearing. Christensen et al. [16] derived a general form of Reynolds equation using the same approach.

In recent years researchers have focused attention on thermohydrodynamic analysis of rough surfaces. A theoretical study of a submerged oil journal bearing was made by Ramesh et al. [17] considering surface roughness and thermal effects. Chang and Farnum [18] developed a thermal model that can be used to analyze the transient elastohydrodynamic lubrication of rough surfaces. Huynh and Loe [19] studied the effects of location and shape of a localized corrugation on the performance of a fixed inclined slider bearing. Ozap and Umur [20] proposed an optimum surface profile design performance by implementing a wavy form of roughness on the pad. Recently Sinha and Getachew [21] numerically analyzed the combined effect of thermal and surface roughness on the performance of an infinitely long slider bearing using stochastic approach. In their study two types of roughness: longitudinal roughness and transverse roughness were considered. The analysis indicated that for parallel sliders some load capacity may be generated due to the combined effect for both types of roughness.

All of the works that has appeared in literature do not seem to conform to the experimental results obtained for parallel sliders. It seems natural that as a consequence of heating, there would be a thermal expansion in asperities and probably a distortion of the slider surface. Thus in this paper the effect of thermal distortion of the slider and asperities on different

Prawal Sinha is with the Department of Mathematics and Statistics, Indian Institute of Technology Kanpur, Kanpur, India (phone: 512-259-7213; fax: 512-259-7500; e-mail: prawal@iitk.ac.in).

Getachew Adamu is with the Department of Mathematics, Bahir Dar University, Bahir Dar, Ethiopia (e-mail: getachewsof@yahoo.com).

Getachew Adamu would like to thank the Federation of Indian Chambers of Commerce and Industry for financial support in the form of CV Raman international visiting fellowship at IIT Kanpur, India.

characteristics of an infinitely tilted pad rough slider bearing is analyzed using stochastic approach.

II. Governing Equations

The geometry for the infinitely long slider bearing analyzed in this paper is shown in Fig. 1. The width of the bearing is assumed to be very large as compared to the distance between the pad and the slider surfaces.

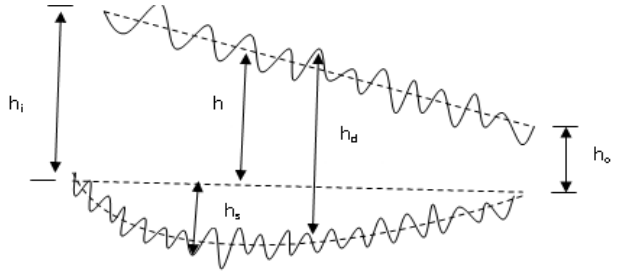

Fig. 1 Schematic diagram of a rough slider bearing after deformation

In view of the usual assumptions of the lubrication theory, Navier -Stokes equations reduced to:

$$\frac{\partial}{\partial y}(\mu\frac{\partial u}{\partial y})=\frac{dp}{dx} \tag{1}$$

and

$$\frac{\partial}{\partial x}(\rho u)+\frac{\partial}{\partial y}(\rho v)=0 \tag{2}$$

Integrating (1) and (2) with the boundary conditions $u=U$, $v=0$ at the slider and $u=v=0$ at the pad and substituting ρ by ρ_{avg} and μ by μ_{avg} leads to the generalized Reynolds type equation:

$$\frac{\partial}{\partial x}\left(\frac{\rho_{avg}H^3}{6\mu_{avg}}\frac{dp}{dx}\right)=U\frac{\partial}{\partial x}\left(\rho_{avg}H\right) \tag{3}$$

where H is the geometry of the fluid film.

The usual lubrication assumptions along with the following assumptions:

- Conduction terms other than those across the fluid film are negligible
- Thermal conductivity and specific heat are constant. lead to a steady state energy equation:

$$\rho c\left(u\frac{\partial T}{\partial x}+v\frac{\partial T}{\partial y}\right)=k_o\frac{\partial^2 T}{\partial y^2}+\mu\left(\frac{\partial u}{\partial y}\right)^2 \tag{4}$$

Viscosity and density are related to temperature via the following relationships:

$$\rho=\rho_a(1-\lambda(T-T_a)),\ \mu=\mu_a\exp(-\beta(T-T_a)) \tag{5}$$

$$\rho_{avg}=\rho_a(1.0-\lambda(T_{avg}-T_a))$$

$$\mu_{avg}=\mu_a\exp(-\beta(T_{avg}-T_a)) \tag{6}$$

In the stochastic theory of an isothermal hydrodynamic lubrication of rough surface bearings developed by Christensen and Tonder [14] and Christensen [15], a Reynolds-type equation in the mean pressure as applicable to rough surface bearings is formulated by considering the film thickness as ergodic (stationary) stochastic process.

In such studies the geometry of the lubricant film $H(x,z,\varepsilon)$ is generally considered to be made up of two parts; the nominal (smooth) part which measures the large scale part of the film geometry including any long wave length disturbances, and a randomly varying quantity with zero mean (arises due to the surface roughness measured from the nominal level). However, due to thermal distortion, the film thickness shall be modified. It is assumed that the distortion leads to a profile of the slider which may be parabolic. Thus the equation of the slider profile may have the following form:

$h_s=K-\frac{4K}{B^2}(x-0.5B)^2$ for some dimensional constant K.

Hence, the lubricant film height is of the form:

$$H(x,z,\varepsilon)=h_d+(1+\alpha)\delta$$

where $h_d=h-h_s$, h is the nominal film height before thermal distortion, α is thermal expansion and δ random roughness variable.

The stochastic theory developed by Christensen and Tonder [14] and Christensen [15] was based on the following additional assumptions:

1. The magnitude of the pressure ripples associated with the surface roughness is small compared with the general pressure level in the bearing, and consequently, the variance of the pressure gradient in the roughness direction is negligible.
2. In the direction perpendicular to the roughness direction the variance of unit flow is negligible.

Sinha and Getachew [21] imposed the following additional assumption to approximate the momentum, continuity and energy equations.

3. The magnitudes of temperature and velocities associated to roughness are small compared to the corresponding general magnitudes in the bearing. Consequently, the variances of ρ , μ , temperature gradient in the direction of roughness, temperature gradient $\frac{\partial T}{\partial y}$ and velocity gradient $\frac{\partial u}{\partial y}$ are negligible.

The theory is applied for two types of one dimensional roughness pattern: longitudinal roughness and transverse roughness. By taking the expected values of both sides of Reynolds equation (3), Sinha and Getachew [21] obtained:

$$\frac{\partial}{\partial x}\left[E\left(\frac{\rho_{avg}H^3}{6\mu_{avg}}\frac{dp}{dx}\right)\right]=U\frac{\partial}{\partial x}E\left(\rho_{avg}H\right) \tag{7}$$

where *E(s)* is the expectancy operator defined by

$$E(s)=\int_{-\infty}^{\infty}sf(s)ds$$

and *f(s)* is the probability density distribution for the stochastic variable s.

Following an approximation process similar to those mentioned by Christensen and Tonder [14], Christensen [15] and Sinha and Getachew [21], the corresponding governing equations are obtained.

The modified Reynolds type equations for longitudinal roughness:

$$\frac{\partial}{\partial x}\left(\bar{\rho}_{avg}\ \frac{1}{\bar{\mu}_{avg}}E\left(H^3\right)\frac{d\bar{p}}{dx}\right)=6U\frac{\partial}{\partial x}\left(\bar{\rho}_{avg}E(H)\right) \tag{8}$$

The modified Reynolds type equations for transverse roughness:

$$\frac{\partial}{\partial x}\left(\bar{\rho}_{avg}\ \frac{1}{\bar{\mu}_{avg}}\frac{1}{E\left(H^{-3}\right)}\frac{d\bar{p}}{dx}\right)=6U\frac{\partial}{\partial x}\left(\bar{\rho}_{avg}\frac{E(H^{-2})}{E(H^{-3})}\right) \tag{9}$$

According to Christensen and et al. [16] and using properties of variance:

$$E\left(H^3\right)=h_d^3+3h_d(1+\alpha)^2\sigma^2,\ \mathrm{E}\left(\mathrm{H}\right)=\mathrm{h}_d$$
$$\frac{1}{E(H^{-3})}=h_d^3-6h_d(1+\alpha)^2\sigma^2 \text{ and}$$
$$\frac{E(H^{-2})}{E(H^{-3})}=h_d\left(1-\frac{3(1+\alpha)^2\sigma^2}{h_d^2}\right)$$

where σ^2 is the variance of the roughness distribution with $\sigma/h_d<<1$. Hence the modified Reynolds equations (8) and (9) can be rewritten respectively as:

$$\frac{\partial}{\partial x}\left(\bar{\rho}_{avg}\ \frac{1}{\bar{\mu}_{avg}}(\mathrm{h}_d^3+3\mathrm{h}_d(1+\alpha)^2\sigma^2)\frac{d\bar{p}}{dx}\right)=6U\frac{\partial}{\partial x}\left(\bar{\rho}_{avg}h_d\right) \tag{10}$$

$$\frac{\partial}{\partial x}\left(\bar{\rho}_{avg}\ \frac{1}{\bar{\mu}_{avg}}(\mathrm{h}_d^3-6\mathrm{h}_d(1+\alpha)^2\sigma^2)\frac{d\bar{p}}{dx}\right)=6U\frac{\partial}{\partial x}\left(\bar{\rho}_{avg}h_d(1-\frac{3(1+\alpha)^2\sigma^2}{h_d^2})\right) \tag{11}$$

Momentum, continuity and energy equations for both kinds of models can be approximated respectively as:

$$\frac{\partial}{\partial y}(\bar{\mu}\frac{\partial\bar{u}}{\partial y})=\frac{d\bar{p}}{dx} \tag{12}$$

$$\frac{\partial}{\partial x}(\bar{\rho}\bar{u})+\frac{\partial}{\partial y}(\bar{\rho}\bar{v})=0 \tag{13}$$

$$\bar{\rho}c\left(\bar{u}\frac{\partial\bar{T}}{\partial x}+\bar{v}\frac{\partial\bar{T}}{\partial y}\right)=k\frac{\partial^2\bar{T}}{\partial y^2}+\bar{\mu}\left(\frac{\partial\bar{u}}{\partial y}\right)^2 \tag{14}$$

The following non-dimensional variables are used:

$$x^*=\frac{x}{B},\ y^*=\frac{y}{h_i},\ \ h^*=\frac{h}{h_i},u^*=\frac{\bar{u}}{U},\ v^*=\frac{\bar{v}B}{Uh_i},$$
$$T^*=\frac{\bar{T}}{T_a},T^*_{avg}=\frac{\bar{T}_{avg}}{T_a},p^*=\frac{\bar{p}h_i^2}{\mu_aUB},p^*{}_i=\frac{\bar{p}_ih_i^2}{\mu_aUB},$$
$$P_e=\frac{\rho_aUch_i^2}{k_oB},\mathrm{Pr}\,Ec=\frac{\mu_aU^2}{k_oT_a},\beta^*=\beta T_a,\lambda^*=\lambda T_a,\alpha^*=\alpha T_a$$
$$\mu^*=\frac{\bar{\mu}}{\mu_a},\mu^*_{avg}=\frac{\bar{\mu}_{avg}}{\mu_a},\rho^*_{avg}=\frac{\bar{\rho}_{avg}}{\rho_a},\ \ \rho^*=\frac{\bar{\rho}}{\rho_a},$$
$$\sigma^*=\frac{\sigma}{h_i},\delta^*=\frac{\delta}{h_i},K^*=K/h_i$$

Non-dimensionalization of the smooth part of the slider profile yields:

$$h_s^*=K^*-4K^*(x^*-0.5)^2$$

Since the parabolic shape of the slider is due to thermal distortion of the slider and the load applied, it is logical to assume that the arc length of the curvature equals to the width of the bearing due to thermal expansion. Using this assumption and the integral arc length formula the non-dimensional equation of the slider profile is approximated to be

$$h_s^*=\sqrt{0.5\alpha^*}(-1+4(x^*-0.5)^2).$$

The non-dimensional forms of the governing equations (10-14) respectively are as follows:

$$\frac{\partial}{\partial x^*}\left(\frac{\rho^*_{avg}(h_d^{*3}+3h_d^*(1+\alpha^*)^2\sigma^{*2})}{6\mu^*_{avg}}\frac{dp^*}{dx^*}\right)= \frac{\partial}{\partial x^*}(\rho^*_{avg}h_d^*) \quad (15)$$

$$\frac{\partial}{\partial x^*}\left(\frac{\rho^*_{avg}(h_d^{3}-6h_d^*(1+\alpha^*)^2\sigma^{*2})}{6\mu^*_{avg}}\frac{dp^*}{dx^*}\right)= \frac{\partial}{\partial x^*}\left(\rho^*_{avg}(h_d^*-\frac{3(1+\alpha^*)^2\sigma^{*2}}{h_d^*})\right) \quad (16)$$

$$\frac{\partial}{\partial y^*}(\mu^*\frac{\partial u^*}{\partial y^*})=\frac{dp^*}{dx^*} \quad (17)$$

$$\frac{\partial}{\partial x^*}(\rho^* u^*)+\frac{\partial}{\partial y^*}(\rho^* v^*)=0 \quad (18)$$

$$\rho^*\left(u^*\frac{\partial T^*}{\partial x^*}+v^*\frac{\partial T^*}{\partial y^*}\right)=\frac{1}{P_e}\frac{\partial^2 T^*}{\partial y^{*2}}+\frac{P_r E_c}{P_e}\mu^*\left(\frac{\partial u^*}{\partial y^*}\right)^2 \quad (19)$$

Fluid boundary conditions:

The boundary conditions for pressure and velocities are:

$$p^*=0 \text{ at } x^*=0,\ p^*=0 \text{ at } x^*=1, u^*=1, v^*=0$$

at the slider,

$$v^*=u^*=0 \text{ at the pad}$$

The boundary conditions associated with the energy equation are:

$$T^*=T_i \text{ at } x^*=0,\ T^*=T_s$$

on the slider and

$$T^*=Tu$$

on the pad, where T_s and T_u are plate temperatures, T_i inlet temperature.

The following three conditions are considered:

a. $T_i=T_s=T_u$

b. $T_u=T_i$ and $T_s=T^*_{avg}$

c. $T_u=T_s=T^*_{avg}$

Condition (a) implies the plate temperatures are constant, conditions (b) and (c) imply that one or both plate temperatures are variable and shall be equal to the average fluid temperature.

III. Formulation of the Problem

To simplify the numerical computation, the irregular domain of the fluid is transformed to regular geometric domain. Assuming the roughness on the pad and the roughness on the runner to be identical random distributions ($\delta_1=\delta_2$), the following linear transformations are used similar to those of Sinha and Getachew [21]:

$$y^*=y'\,h_d^*+h_s^*+(1+\alpha^*)\delta_1^*,\quad 0\le y'\le 1 \quad x^*=x'$$

These transformations will map the lower boundary of the fluid on to $y'=0$ and the upper boundary of the fluid on to $y'=1$.

Using these transformations the governing equations can be rewritten as follows:

$$\frac{\partial}{\partial x'}\left(\frac{\rho^*_{avg}(h_d^{*3}+3h_d^*(1+\alpha^*)^2\sigma^{*2})}{6\mu^*_{avg}}\frac{dp^*}{dx'}\right)=\frac{\partial}{\partial x'}(\rho^*_{avg}h_d^*) \quad (20)$$

$$\frac{\partial}{\partial x'}\left(\frac{\rho^*_{avg}(h_d^{*3}-6h_d^*(1+\alpha^*)^2\sigma^{*2})}{6\mu^*_{avg}}\frac{dp^*}{dx'}\right)= \frac{\partial}{\partial x'}\left(\rho^*_{avg}(h_d^*-\frac{3(1+\alpha^*)^2\sigma^{*2}}{h_d^*})\right) \quad (21)$$

$$\frac{1}{h_d^{*2}}\frac{\partial}{\partial y'}(\mu^*\frac{\partial u^*}{\partial y'})=\frac{dp^*}{dx'} \quad (22)$$

$$\frac{\partial}{\partial x'}(\rho^* u^*)-\frac{1}{h_d^*}\left(\frac{y'dh_d^*}{dx'}+8\sqrt{0.5\alpha^*}(x'-0.5)\right)\frac{\partial}{\partial y'}(\rho^* u^*)+\frac{1}{h_d^*}\frac{\partial}{\partial y'}(\rho^* v^*)=0 \quad (23)$$

$$\rho^*\left(u^*\left(\frac{\partial T^*}{\partial x'}-\frac{1}{h_d^*}\left(\frac{y'dh_d^*}{dx'}+8\sqrt{0.5\alpha^*}(x'-0.5)\right)\frac{\partial T^*}{\partial y'}\right)+v^*\frac{1}{h_d^*}\frac{\partial T^*}{\partial y'}\right)= \frac{1}{h_d^{*2}P_e}\frac{\partial^2 T^*}{\partial y'^2}+\frac{P_r E_c}{h_d^{*2}P_e}\mu^*\left(\frac{\partial u^*}{\partial y'}\right)^2 \quad (24)$$

The corresponding non dimensional density and viscosity relationships in the new coordinate system are:

$$\rho^*=1.0-\lambda^*(T^*-1.0),\quad \mu^*=\exp(-\beta^*(T^*-1.0)) \quad (25)$$

$$\rho^*_{avg}=1.0-\lambda^*(T^*_{avg}-1.0),\quad \mu^*_{avg}=\exp(-\beta^*(T^*_{avg}-1.0)),\ \text{where } T^*_{avg}=\int_0^1 T^*dy' \quad (26)$$

The non dimensional load carrying capacity W^* and the friction force F^* are determined from the following expressions respectively:

$$W^* = \frac{Wh_i^2}{\rho_a UB^2} = \int_0^1 p^* dx' \quad (27)$$

$$F^* = \frac{Fh_i}{\mu_a UB} = \int_0^1 (\mu^* \frac{\partial u^*}{h_d^* \partial y})_{y'=0} dx' \quad (28)$$

IV. Treatment of the Solution

The system of equations was discretized and solved simultaneously using finite difference technique. Backward difference is used for the derivatives $\frac{\partial v^*}{\partial y'}$ in the continuity equation and $\frac{\partial T^*}{\partial x'}$ in the energy equation. For all other derivatives central difference is used except at the boundaries. Appropriate one sided difference is used at the boundaries.

A direct iterative approach was used to obtain the distributions of all field variables. At every iteration level, the governing equations are solved in a decoupled form.

The results have been obtained to an accuracy of $Tol=10^{-6}$, where

$$\max\left(\frac{|\zeta_j^{new} - \zeta_j old|}{|\zeta_j^{new}|}\right) \le Tol, \quad \zeta_j$$

are the field variables.

The iteration is carried out for $Tol=10^{-5}$, $Tol=10^{-6}$, $Tol=10^{-7}$ and there is no significant difference in the values.

A. Algorithm

In the computational work, two stages of computations are used. In the first stage all the field variables and average temperature across the film are approximated using $\alpha^*=0$ and prescribed constant slider temperature T_s (before thermal distortion is taking place). In the second stage the equations are solved using non-zero α^* and slider temperature $T_s = T^*_{avg}$ taking the values obtained from stage one as initial data for the variables.

Step 1. Initialization

a Input data:

k_o, B, $\lambda^*, \beta^*, \sigma^*, h_i^*, P_r, E_c, P_e, \alpha^* = 0$

b Set boundary conditions for u^*, v^*, T^*, p^*

c Set fictitious values for u^*, v^*, T^*, p^* to the remaining grid points

Step 2. Evaluate p^{*new} using ρ^{*old}_{avg}, μ^{*old}_{avg}, T^{*old}_{avg}

Step 3. Evaluate u^{*new} using p^{*new}, T^{*old}

Step 4. Evaluate v^{*new} using u^{*new} and T^{*old}

Step 5. Evaluate T^{*new} using, $p^{*new}, u^{*new}, v^{*new}$, T^{*old}

Step 6. Evaluate: $T^{*new}_{avg}, \rho^{*new}, \mu^{*new}, \rho^{*new}_{avg}, \mu^{*new}_{avg}$ using T^{*new}

Step 7. Test for convergence.

Step 8. Repeat steps 2-7 till convergence is obtained.

Step 9. Set an appropriate non zero α^* and reset the thermal boundary conditions in terms of T_i and T^*_{avg}

Step 10. Repeat steps 2-9 till $\frac{|T^{*new}_{avg} - T^{*old}_{avg}|}{|T^{*new}_{avg}|} < Tol$

Step 11. Calculate load capacity W^* and friction force F^*.

V. Results and Discussion

In the present study the values of the following parameters are chosen.

U=20 m/s, h_i=0.00005m, B=0.1m, c=1926J/kg K, T_a=310K, ρ_a=897.1kg/m^3, μ_a=0.0174pa.s, β=0.035/K, λ=0.0012/K, ko=0.132 W/(mK), α =13 m/(mK).

The simulation has been carried out for various values of m, λ^*, β^* and σ^* with fixed values of the parameters α, P_e, P_r and E_c. The effect of roughness is felt only through $h_o/3\sigma$, where h_o is the minimum film thickness [14]. The roughness effects are not important if $h_o >> 3\sigma$. However, when $h_o \approx 3\sigma$ (within the hydrodynamic limit i.e $h_o > 3\sigma$) the influence on the bearing performance is significant. For comparison purposes, the roughness parameter σ^* is fixed at 0.1 which is 25% and 10% of the minimum film thickness for m=0.4 and m=1.0(parallel sliders) respectively. Also λ^* =0.4 is fixed for the same. The performance of the bearing is observed for different values of β^* (β^*=1.0, 5.0, 10.0).

The results have been analyzed, for pressure distribution, load capacity, friction force and temperature. The results are presented in the form of graphs and tables. To ensure the grid independence of the results, the numerical simulations are carried out on different grid systems consisting of 10x10, 20x20, 30x30 and 40x40 grid points. The load capacities of the bearings obtained using different grids have been compared and presented in Fig. 2. From this figure it can be concluded that the 40x40 grid system yields a grid independent solution.

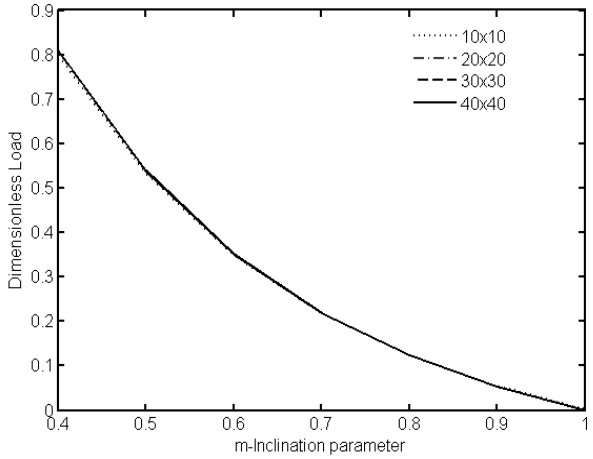

Fig. 2 Dimensionless load capacity versus inclination parameter for different grids systems

In the results that follow, emphasis has been given to the following three cases of thermal boundary conditions:

Case.i Before distortion($T_i = T_s = T_u$)

Case.ii After distortion ($T_u = T_i$ and $T_s = T^*_{avg}$)

Case.iiiAfter distortion ($T_u = T_s = T^*_{avg}$)

As a consequence of thermal distortion the following situations may occur in the bearing:

- The fluid temperature rises (Fig. 3) which in turn reduces the fluid viscosity. Consequently the pressure may decrease and this may lead to a reduction in the load capacity.
- The average thickness may increase (due to the parabolic profile of the slider). The increased volume inside the bearing may result in a decrease of flow pressure and hence in a decrease of load capacity (see Fig. 1)
- The asperities of both surfaces may be distorted. Because of this the average film thickness may be decreased and hence the load capacity is likely to be enhanced.

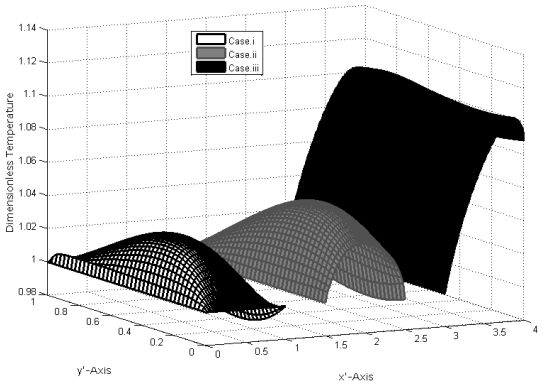

Fig. 3 Dimensionless temperature distributions for transverse roughness (m=0.4, T_i=1.0)

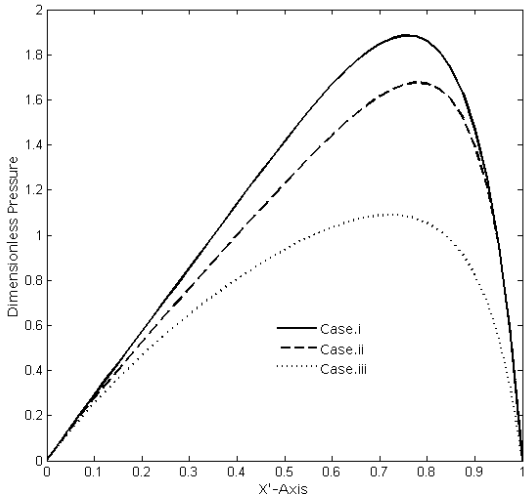

Fig. 4 Dimensionless pressure distributions for transverse roughness (m=0.4, T_i=1.0)

The total sum effect of the above conditions on pressure and temperature distributions are shown in Figs. 3 and 4 respectively. From Fig. 3 one can easily observe that the bearing temperature distributions are higher in Cases.ii and iii as compared to that for Case.i. From Fig. 4 the pressure distributions for Cases.ii and iii are less than that for Case.i. For non-parallel bearings (m=0.4) the load capacity decreases by 11% for longitudinal roughness and by 12% for transverse roughness for Case ii , and by 47 % for longitudinal and56 % for transverse roughness for Case iii as compared to that for Case i (see Fig. 5 and Tables I, II). Whereas, for parallel bearings (m=1.0) the load capacity is generated and increases by 7% for Case.ii and more than 50% for Case.iii as compared to that for Case. i, for both types of surface roughness (see Fig. 6 and Tables I, II). From this, one can conclude that the thermal expansion of the fluid and the bearing asperities may be one of the most important factors for load capacity generation in parallel bearings.

For m=0.4 the friction force decreases by 15% for Case.ii and by more than 50% for Case.iii for both types of roughness as compared to that for Case.i. Unlike the load capacity the friction force decreases by 7% and 18% for Cases.ii and iii as compared to that for Case.i, respectively for parallel bearings (see Tables I, II). It is because the viscosity of the fluid decreases due to temperature rise in the fluid (see Fig. 6). From the above it can be seen that the thermal distortion effects are less for Case.ii compared to that for Case.iii. Thus, it is possible to improve the performance of the bearing by cooling the pad even when thermal distortion takes place.

In the Tables I and II, Q_1 and Q_2 are defined as follows:

$$Q_1 = \left|\frac{\text{Case.i} - \text{Case.ii}}{\text{Case.ii}}\right|, \quad Q_2 = \left|\frac{\text{Case.i} - \text{Case.iii}}{\text{Case.iii}}\right|$$

TABLE I
LOAD CAPACITY AND FRICTION FORCE DISTRIBUTIONS FOR LONGITUDINAL ROUGHNESS (B*=10, Σ*=0.1)

m	T_i		Case.i	Case.ii	Q_1%	Case.iii	Q_2%
0.4	1	W*	0.810618	0.733274	11	0.550455	47
		F*	1.582893	1.378491	15	0.95897	65
	1.1	W*	0.320297	0.300133	7	0.255736	25
		F*	0.625716	0.576013	9	0.471121	33
	1.2	W*	0.121313	0.115433	5	0.106391	14
		F*	0.237074	0.223795	6	0.203211	17
1.0	1	W*	0.001687	0.001839	8	0.003864	56
		F*	0.933435	0.871956	7	0.790967	18
	1.1	W*	0.000265	0.000304	13	0.000706	62
		F*	0.361855	0.345691	5	0.331033	9
	1.2	W*	0.000039	0.000041	5	0.000113	65
		F*	0.135884	0.130938	4	0.128694	6

TABLE II
LOAD CAPACITY AND FRICTION FORCE DISTRIBUTIONS FOR TRANSVERSE ROUGHNESS (B*=10, Σ*=0.1)

m	T		Case.i	Case.ii	Q_1%	Case.iii	Q_2%
0.4	1	*W**	1.134857	1.016186	12	0.725157	56
		*F**	1.658952	1.436445	15	0.898316	84
	1.1	*W**	0.450209	0.422703	7	0.355503	26
		*F**	0.651177	0.595621	9	0.45842	42
	1.2	*W**	0.1709	0.164147	4	0.154614	11
		*F**	0.246735	0.233044	6	0.205212	20
1	1	*W**	0.001793	0.001932	7	0.004128	56
		*F**	0.933422	0.87207	7	0.791021	18
	1.1	*W**	0.000282	0.00032	11	0.00065	56
		*F**	0.361851	0.345699	5	0.331182	9
	1.2	*W**	0.000041	0.000043	5	0.000125	67
		*F**	0.135882	0.130937	4	0.128694	6

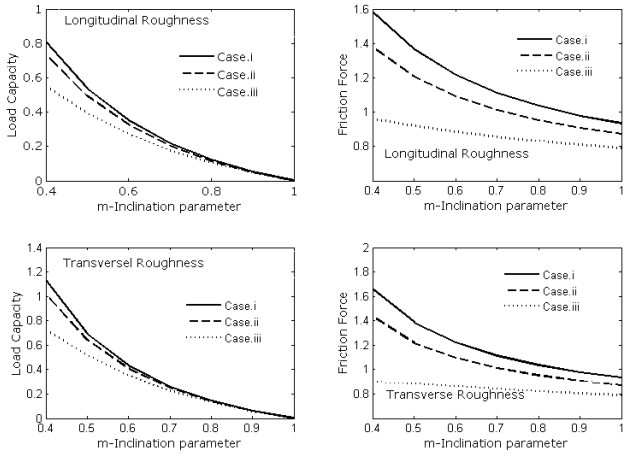

Fig. 5 Load capacities and friction forces for both types of roughness (m=0.4, T_i=1.0)

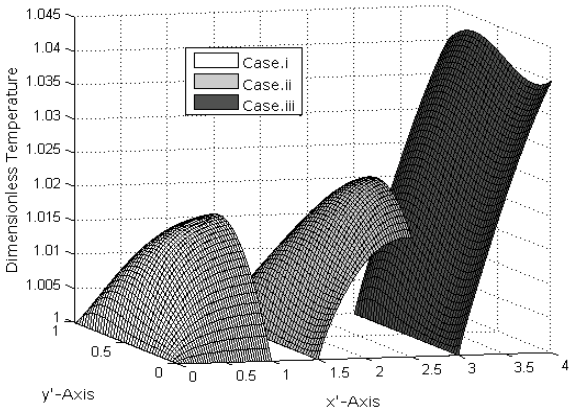

Fig. 6 Dimensionless temperature distributions for transverse roughness (m=1.0, T_i=1.0)

Tables III and IV show the load capacity and friction force distributions for two values of thermal coefficient in viscosity formula (β=1.0, 5.0).For both values of β the load capacity of parallel bearing is increased for both types of roughness for Cases.ii and iii as compared to that for Case.i. It is also observed that for β=1.0 the load capacity of non- parallel bearing is increased for transverse roughness for Cases.ii and iii as compared to that for Case.i though small. From the tables one can also observe that the effects of thermal distortion with β=1.0, 5.0 are less compared to the effects of thermal distortion with β=10.0.

TABLE III
LOAD CAPACITY AND FRICTION FORCE DISTRIBUTIONS FOR LONGITUDINAL ROUGHNESS (Σ*=0.1)

m	*Ti*		β=1.0			β=5.0		
			Case.i	Case.ii	Case.iii	Case.i	Case.ii	Case.iii
0.4	1	*W**	0.895921	0.859046	0.848792	0.854941	0.796079	0.669989
		*F**	1.759031	1.671508	1.568962	1.673613	1.520424	1.19623
	1.1	*W**	0.811673	0.77799	0.769007	0.531299	0.500307	0.440742
		*F**	1.59361	1.515962	1.426974	1.039714	0.963603	0.809722
	1.2	*W**	0.73527	0.704514	0.697476	0.327266	0.310578	0.283338
		*F**	1.443588	1.374385	1.297524	0.640268	0.601551	0.601551
1	1	*W**	0.001996	0.003253	0.008094	0.001848	0.002558	0.005834
		*F**	1.007388	0.973182	0.960352	0.972787	0.924767	0.87386
	1.1	*W**	0.001694	0.00281	0.007112	0.00073	0.001037	0.002487
		*F**	0.91221	0.881463	0.870304	0.599958	0.574525	0.552989
	1.2	*W**	0.001438	0.002403	0.006277	0.000284	0.000404	0.001034
		*F**	0.825975	0.798395	0.788673	0.367716	0.353948	0.353948

TABLE IV
LOAD CAPACITY AND FRICTION FORCE DISTRIBUTIONS FOR TRANSVERSE ROUGHNESS (B*=10, Σ*=0.1)

m	***Ti***		β=1.0			β=5.0		
			Case.i	Case.ii	Case.iii	Case.i	Case.ii	Case.iii
0.4	1	*W**	1.260287	1.208933	1.227395	1.199058	1.109232	0.910307
		*F**	1.830374	1.7388	1.601719	1.742508	1.56958	1.152221
	1.1	*W**	1.142047	1.098967	1.12572	0.746741	0.704758	0.617562
		*F**	1.658417	1.578131	1.459962	1.08171	0.997413	0.795686
	1.2	*W**	1.034769	0.998841	1.029391	0.46063	0.440036	0.407334
		*F**	1.502429	1.431701	1.32994	0.66623	0.625933	0.531966
1	1	*W**	0.002121	0.003494	0.009203	0.001963	0.002735	0.006459
		*F**	1.007379	0.973145	0.960216	0.972774	0.92479	0.873787
	1.1	*W**	0.0018	0.003035	0.008314	0.000776	0.000997	0.002823
		*F**	0.912203	0.881437	0.870164	0.599951	0.997413	0.552971
	1.2	*W**	0.001527	0.002628	0.007449	0.000302	0.000424	0.00119
		*F**	0.825967	0.798365	0.788534	0.367712	0.353947	0.34504

For different values of inlet temperature T_i the thermal distortion effects are given in the Tables I-IV. From these tables one can observe that as the inlet temperature increases the thermal distortion effect on the performance of the bearing decreases (see Figs. 5 and 7)

VI. CONCLUSION

The stochastic approach for hydrodynamic lubrication for rough surface bearings is extended to the study of thermo-hydrodynamic lubrication of rough surface bearings considering thermal distortion of the slider and asperities. For both roughness models, it is seen that the load carrying capacity and friction force are decreased due to thermal distortion for non parallel bearings. For parallel bearings the load capacity is enhanced and friction force is decreased due to thermal distortion of the slider and asperities. It is also observed that for both models, the effects of thermal distortion for Case.ii are less compared to that for Case.iii. From this one can concluded that cooling the pad can improve the performance of the bearing. Moreover the effect of thermal distortion is more pronounced in the case of low inlet temperatures.

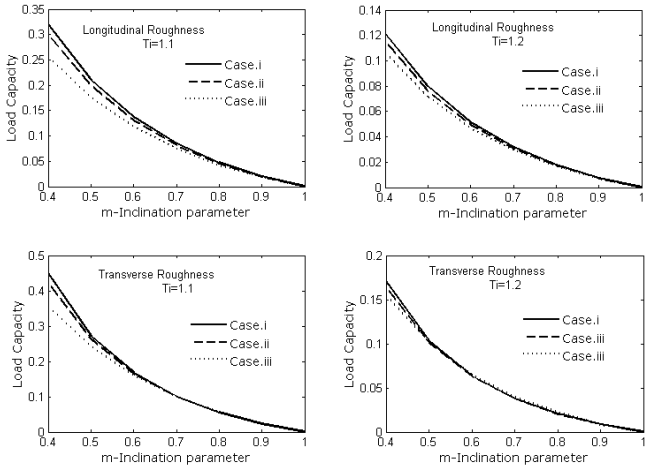

Fig.7 Load Capacity for both types of roughness with different inlet temperatures (T_i=1.1 and T_i=1.2)

NOMENCLATURE

B	bearing width
c	specific heat of lubricant
E_c	Eckert number
E	expected value operator
F	frictional drag force
h	nominal film thickness
h_i	nominal film thickness at the leading edge
h_o	nominal film thickness at the trailing edge

H	the height of the film for rough surface
k_0	thermal conductivity of the lubricant
m	h_o/h_i
p	film pressure
P_e	Peclet number
p_i	inlet pressure
P_r	Prandtl number
T	lubricant temperature
Tu, T_s	temperatures of plates
T_i	inlet temperature
u,v	fluid velocities
U	velocity of the moving surface
x, y	coordinate system
x', y'	transformed coordinate system
W	load carrying capacity of the bearing
A	thermal expansion coefficient
β	temperature coefficient in viscosity formula
δ	random distributions of roughness
ε	random variable
λ	temperature coefficient in density formula
μ	viscosity of the lubricant
ρ	density of the lubricant
σ^2	variance of roughness

Super script * depicts a corresponding non dimensional quantity and bar above a variable depicts the corresponding expected value. The suffix 'a' in a variable indicates the ambient value and the suffix 'avg' indicates the average value across the film of the corresponding quantity.

REFERENCES

[1] A. Fogg, "Fluid Film Lubrication of Parallel Thrust Surfaces." *In: Proc. Inst. Mech. Eng.*, vol.155**,** pp. 49-53, 1946.

[2] F. Osterle, A.Charnes and A.Saibel, "On the Solution of the Reynolds Equation for Slider Bearing Lubrication-IV- The Parallel Surface Slider Bearing without Side Leakage," *Trans. ASME*, pp. 1133-1136, 1953.

[3] W. Lewicki, "Theory of Hydrodynamic Lubrication in Parallel Sliding," *Engnr., London* 200, pp. 939-941, 1955.

[4] A. Cameron, "The viscosity Wedge," *Trans. ASME* vol. 1, pp. 248-253, 1958.

[5] J. Young, "The Thermal Wedge in Hydrodynamic Lubrication," *Eng. J.* vol. 45, pp. 46-54, 1962.

[6] A.O. Lebeck, "Parallel Load Support in the Mixed Friction Regime, Part I-The Experimental Data," *Trans. ASME, J. Trib*. Vol. 109, pp.189-195, 1987.

[7] O.C. Zienkiewicz, "Temperature distribution within lubricating films between parallel bearing surfaces and its effect on the pressures developed." *In: Proc. of conference on lubrication and wear*, paper No. 7, Inst. Mech. eng., London, 1957.

[8] C.M. Rodkiewicz, Prawal Sinha, "On the Lubrication Theory: A Mechanism Responsible for Generation of the Parallel Bearing Load Capacity," *Trans. ASME, J. Lub. Tech*. vol.115, pp. 584-590, 1993.

[9] H. Ezzat, S. Rhode, "A Study of Hydrodynamic Performance of Finite Slider Bearings," *Trans. ASME, J. Lub. Tech*. vol.95, 3, pp. 298-307, 1973.

[10] O. Pinkus, "Thermal Aspects of Fluid Film Tribology," *ASME Press*, New York, 1990.

[11] B.V.Rathish, P.S.Rao, and P.Sinha, "Stream Line Upwind Petrov-Gaerkin Finite Element Analysis of Thermal Effects on Load Carrying Capacity in Slider Bearings," *Num. Heat Transfer. Part A: Applications* vol.38, pp.305-328, 2000.

[12] M.M. Khonsari, "A Review of Thermal Effects in Hydrodynamic Bearings. Part I: Slider/Thrust Bearings, Part II:" *Journal Bearings, ASLE Trans*. Vol. 30, pp. 19-33, 1987.

[13] S.T.Tzeng, H.Saibel, "Surface Roughness Effect on Slider Bearing Lubrication," *ASME Trans*. Vol. 10, pp. 334-338, 1967.

[14] H. Christensen, K. Tonder, "Tribology of Roughness: Stochastic Models of Hydrodynamic Lubrication," *SINTEF report* 10/69-18, 1969.

[15] H. Christensen, "Stochastic Models of Hydrodynamic Lubrication of Rough Surfaces." *In: Proc. Inst. mech. Eng*. Vol. 184, pp.1013-1022, 1969-70.

[16] H. Christensen, J.B. Shukla, and S. Kumar, "Generalized Reynolds Equation for Stochastic Lubrication and its Application," *J, Mech. Eng. Sci*. vol. 17, pp. 262-270, 1975.

[17] J. Ramesh, C. Majumdar, and N.S. Rao, "Thermohydrodynamic Analysis of Submerged Oil Journal Bearings Considering Surface Roughness Effects," *Trans. ASME, J. Trib*. Vol. 119, pp. 100-106, 1997.

[18] L. Chang, C. Farnum, "A Thermal Model for Elastohydrodynamic Lubrication of Rough Surfaces," *Tribology Trans*. Vol. 35, pp. 281-286, 1992.

[19] B.P. Huynh, S. Loe, "Influence of Location, Number and Shape of Corrugations in Slider Bearings," *Anziam J*. vol. 45, pp. C1017-C1038, 2004.

[20] A.A. Ozap, H. Umur, "Optimum Surface Profile Design and performance Evaluation of Inclined Slider Bearings," *Current Science*, vol. 90, pp. 1480-1491, 2006.

[21] Sinha Prawal, A. Getachew, "THD analysis for slider bearing with roughness: special reference to load generation in parallel sliders," *Acta Mechanica*, vol. 207**,** Issue 1, pp 11, 2009.